

Performance Improvement of Dye-Sensitized Solar Cells with AZO and BZO Blocking Layers

Kenan Ozel^{1,2,*}, İlhan Kosalay³, Abdullah Atılğan², Aycan Atlı², Z. Kerem Yıldız² and Abdullah Yıldız²

¹Gama Vocational School, Ankara University, Ankara, Turkey

²Department of Energy Systems Engineering, Faculty of Engineering and Natural Sciences, Ankara Yıldırım Beyazıt University, Ankara, Turkey

³Department of Electrical and Electronics Engineering, Faculty of Engineering, Ankara University, Ankara, Turkey

Received: April 03, 2018, Accepted: July 17, 2018, Available online: December 25, 2018

Abstract: In this work, studies were made to improve the photoelectrical characteristics of the dye-sensitized solar cells (DSSCs) with undoped and Al, B doped ZnO blocking layers (BLs) placed at the interface of SnO₂:F (FTO) material and porous TiO₂ layer. The BLs were prepared by sol-gel method and deposited onto FTO surface by using spin coating technique. TiO₂ paste was applied onto the blocking layer by Doctor Blade method to form the working electrodes (WEs) of the DSSCs. Wild jasmine (*Jasminum fruticans*) and mahaleb cherry fruit (*Prunus mahaleb*) extracts were used to sensitize the porous TiO₂ layer. Our findings demonstrated that the application of Al and B-doped ZnO BLs between TiO₂ layer and FTO improves the solar photovoltaic electrical characteristics.

Keywords: Blocking layer; Dopant; Natural dye; Dye-sensitized solar cell

1. INTRODUCTION

DSSCs have attracted lots of interest since they were first announced by O' Regan and Graetzel in 1991 [1]. They might offer good alternatives to conventional solar cells due to their low production cost, easy fabrication and high efficiencies. A typical DSSC is made up of a transparent conductive oxide layer (FTO/ITO), a semiconductor layer called photoanode, a light sensitive dye, an ionic electrolyte and Pt-coated FTO as counter electrode [2]. In recent years, various techniques have been used to enhance their photovoltaic performance [3]. In DSSCs, the morphological and structural characteristics of semiconductor layer, interfacial resistances and recombination of electron-hole pairs are some factors affecting the performance of the cell [4]. Many efforts have been made to determine the effects of these factors. One method to overcome the degradation in performance is to add a BL in the interface between FTO and semiconductor layer [5].

Liu *et al.* [6] reported that the existence of a BL at the interface FTO/TiO₂ decreases the carrier recombination and inhibits back electron transfer. They showed that ZnO BL significantly contributes to the performance of DSSCs. It reduces not only interfacial charge recombination but also improves adherence of porous TiO₂ to FTO. Moreover, adding such a layer creates an

energy barrier which enhances the efficiency of DSSC. Nb₂O₅ [7], TiO₂ [8], ZnO [9] and MgO [10] have been considered as BLs before. Among these metal oxides, ZnO BL receives extensive attentions because it possesses superior optical and electrical properties [11]. Also, it exhibits an obvious improvement of electron density in the conduction band of TiO₂ due to low conduction band level [6].

On the basis of the information above, we report on the preparation of undoped, Al and B doped ZnO BLs deposited onto the FTO. The effect of natural dyes on the performance of DSSCs is also investigated.

2. EXPERIMENTAL

In the study, Zinc acetate dihydrate (ZAD) (≥ 98.0%, Merck) as precursor, ethanol (≥99.9%, Merck) as solvent and monoethanolamine (MEA) (99.5%, Merck) as stabilizer were used in the synthesis of BL solutions by sol-gel method. Also, precursors such as Aluminum nitrate nanohydrate (98%, Sigma Aldrich) for Aluminum and Trimethyl borate (98%, Sigma Aldrich) for Boron were utilized to obtain dopant atoms. TiO₂ (Degussa P25 nanopowder), Acetic acid (99.8%, Sigma-Aldrich), Terpinol (95%, Sigma- Aldrich), and an ethyl cellulose stock solution were employed to form TiO₂ paste [12].

The blocking layer solutions were adjusted to have a molarity of 0.2 M (mol / L) with a doping ratio of 2 at%. After being aged,

*To whom correspondence should be addressed: Email: kozel@ankara.edu.tr

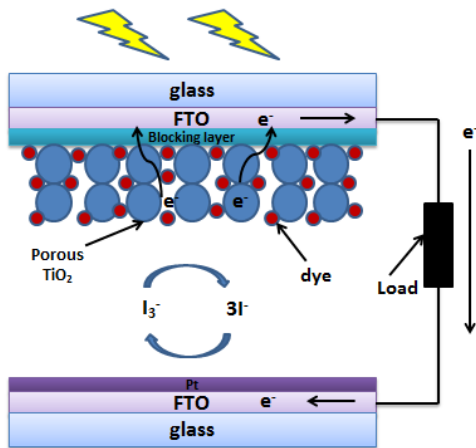


Figure 1. The schematic view of the DSSC with ZnO

prepared blocking layer solutions were spin-coated on the clean FTO glass substrate at a speed of 2000 rpm for 30s. The ZnO:X (X:Al, B)/FTO structure were dried for 20 min and then annealed at 500°C for 5 min to obtain films with AZO or BZO BL. The edges of ZnO:X (X:Al, B)/FTO structure were taped with Scotch 3M tape to get TiO₂ semiconductor layer with the same thickness. Then TiO₂ paste was coated on these structure by doctor blading technique. The coated films were kept at room temperature and sintered at 500°C to acquire a porous TiO₂ structure called photoanode.

Wild jasmine (*Jasminum fruticans*) and mahaleb cherry fruits (*Prunus mahaleb*) were extracted and filtered then diluted with a 20% ethanol solution to obtain natural dye solutions. The TiO₂/ZnO:X (X:Al, B)/FTO structures were soaked into the dye solution for 18 hours so that the porous TiO₂ semiconductor layer could absorb enough dye. The iodide / tri-iodide electrolyte solution, which hosts to reduction-oxidation reaction of DSSCs, was prepared using 0.05 M Iodine (I₂) (≥99.8%, Sigma-Aldrich), 0.5 M Lithium iodide (LiI) (≥ 98.0%, Merck), and Acetonitrile (99.9%, Sigma-Aldrich). Iodine and Lithium iodide were separately mixed in acetonitrile for 24 hours in a magnetic stirrer until they dissolved and then combined to prepare a liquid ionic electrolyte solution. Platisol T / SP (Solaronix, Switzerland) was deposited onto FTO to have a counter electrode. Dye-loaded porous TiO₂ samples called working electrodes, which have Natural Dye/ TiO₂/ ZnO:X (X:Al, B)/FTO structure, and Pt-coated counter electrodes were assembled to fabricate DSSC by injecting liquid electrolyte between these electrodes (see Fig. 1).

X-ray diffraction measurements were conducted to confirm the formation of TiO₂ and doped ZnO on the FTO with Rigaku Miniflex 600 XRD. The surface roughness of the TiO₂/ ZnO:X (X:Al, B)/FTO paste structures was investigated using Quesant Ambios Atomic Force Microscope (AFM). The optical absorbance values of samples before and after dye-loading were collected with Shimadzu Corporation UV-vis spectrophotometer at the wavelength from 400 nm to 800 nm. Finally, Current density – Voltage characteristics of prepared sandwich-type DSSCs were obtained with an *I-V* measurement system under AM 1.5 one sun illumination. Also, external solar cell parameters i.e., that short circuit current (*I_{sc}*), open circuit voltage (*V_{oc}*) and fill factor (*FF*) were determined.

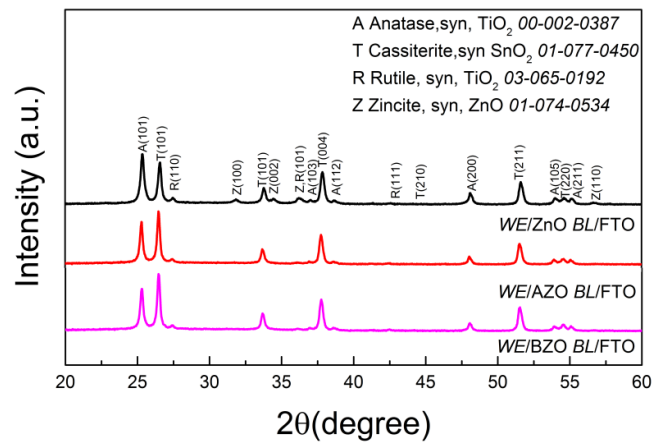


Figure 2. X-ray diffraction pattern of the WEs

3. RESULTS AND DISCUSSION

Fig. 2 shows the XRD pattern of the WEs. The WEs have polycrystalline structure, whose dominant phase is anatase. While the anatase and rutile phases come from TiO₂ layer, cassiterite phase is caused due to SnO₂ of the FTO coated glass substrate. In addition, some peaks have zincite phase as the reflection of ZnO BLs. The average crystallite size of the films was determined using the Debye-Scherrer formula given as the following [13],

$$D = \frac{(0.9\lambda)}{\beta \cos\theta} \quad (1)$$

where λ refers to the wavelength of the X-rays (0.154 nm), β indicates full width at half maximum (FWHM) and θ is the diffraction angle which belongs to (A101) peak position. The estimated value of *D* is 25, 29 and 28 nm for WEs on ZnO, AZO and BZO, respectively. After doping, it can be observed that the largest Bragg peak occurs in (101) direction for the cassiterite phase from the FTO. The decrease in intensity of ZnO related peaks might be due to intercorporation of dopant atoms into the ZnO lattice [14]. Furthermore, the peak positions are slightly shifted because of the smaller ionic radius of Al and B atoms than that of Zn atoms. This indicates that dopant atoms successfully introduced into ZnO lattice [15]. In addition, the crystallite sizes of the WEs with AZO and BZO BLs are larger than the WE with undoped ZnO BL [16].

The surface images of the WEs are investigated by AFM measurements. Fig. 3 shows the surface morphology of the films. The root-mean square (RMS) roughness of these electrodes are approximately 137, 470 and 89 nm for WEs with ZnO, AZO, BZO BL, respectively. Surface roughness of the films is directly related with the adhesion of the layers [17]. In fact, high surface roughness may lead to decrease in interfacial resistance, providing better contact between porous TiO₂ and FTO [18]. In addition, a higher RMS value means large surface area. Large surface area allows the porous structure to absorb more dye and so, improves the number of photo-generated electrons. *FF* and *V_{oc}* are affected by these electrons [19]. Also, low interfacial resistance and high surface area for porous structure positively contribute to the photovoltaic performance of DSSCs [18].

The absorption profiles of the WEs before dye loading are shown in Fig. 4a. The absorption spectra of the films exhibits a peak at 426 nm (AZO) and 436 nm (BZO). It stands for the values

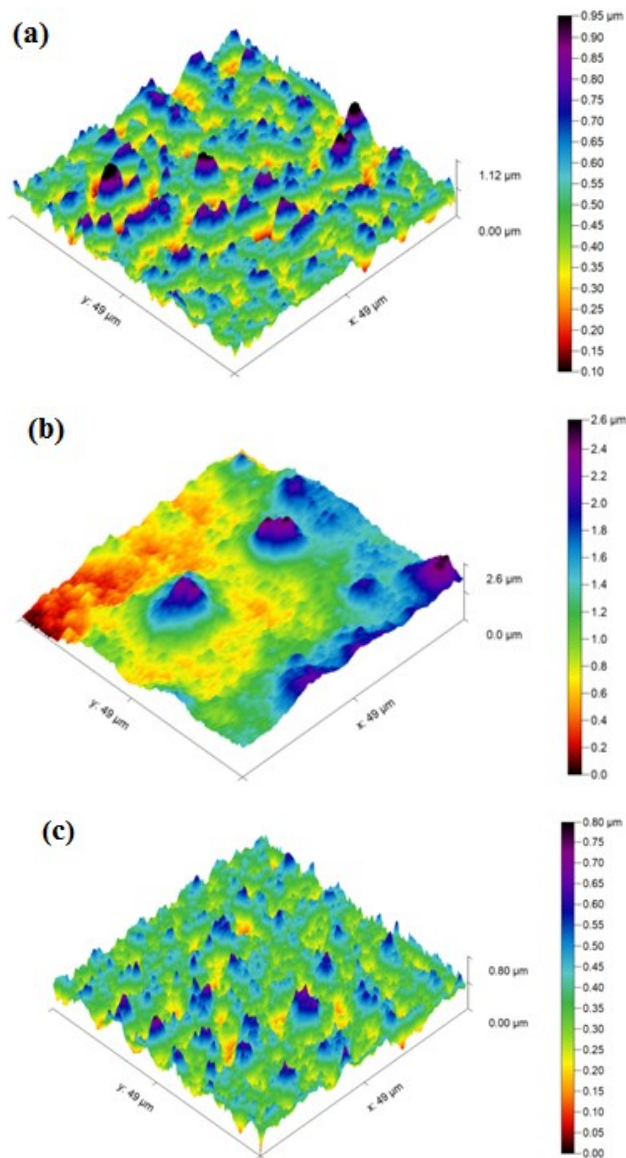


Figure 3. Three-dimensional AFM images of working electrodes with (a) ZnO BL (b) AZO BL (c) BZO BL

of band gap of 2.91 and 2.84 eV for *WEs* with AZO and BZO BL, respectively. The optical characteristics of the FTO/BL/TiO₂ structures sensitized with wild jasmine (dye-1) and mahaleb cherry fruit (dye-2) are shown in figures 4b and 4c. Dye loading causes a slight red-shift to long wavelength region. Improved absorption profiles of *WEs/BL* allow cells to benefit from more photons. In addition, extended absorption region results in higher short circuit current density (J_{sc}). Different BLs and natural dye types have different absorption characteristics. This is because the natural dyes contain different types of anthocyanins and have different color pigments [20].

The photocurrent density (J_{sc})–voltage (V) characteristics of the DSSCs are represented in figures 5a and 5b. Also, the performance parameters for the cells such as J_{sc} , V_{oc} , FF are given in Tables 1 and 2 for different dyes. From the slopes of J - V curves, series

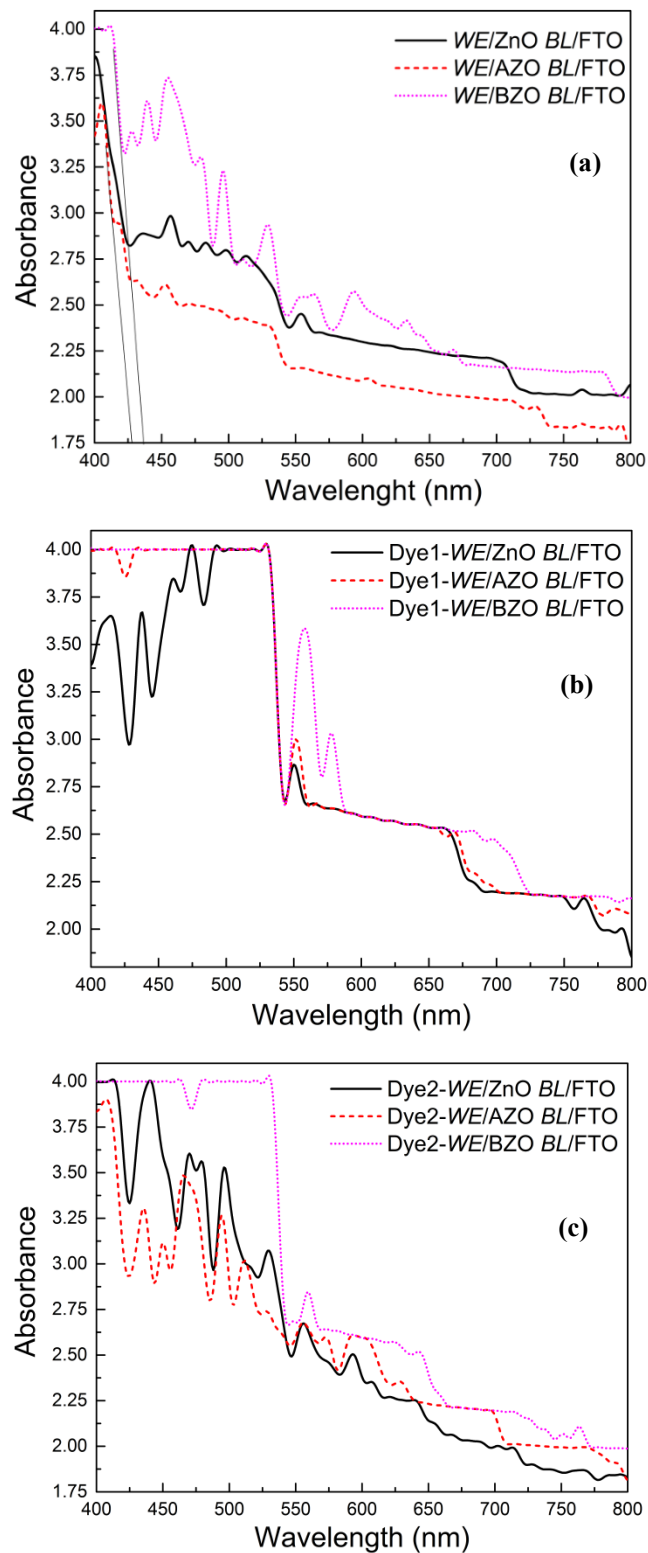


Figure 4. (a) UV-vis absorption spectra of the FTO/BL / TiO₂ structure before dye sensitization, (b) UV-vis absorption spectra of the FTO / BL / TiO₂ structure sensitized with wild jasmine (dye1), (c) UV-vis absorption spectra of the FTO / BL / TiO₂ structure sensitized with mahaleb cherry fruit (dye2)

resistance (R_s) and shunt resistance (R_{sh}) are extracted.

As can be observed from $J-V$ figures, the R_s value of the cell with

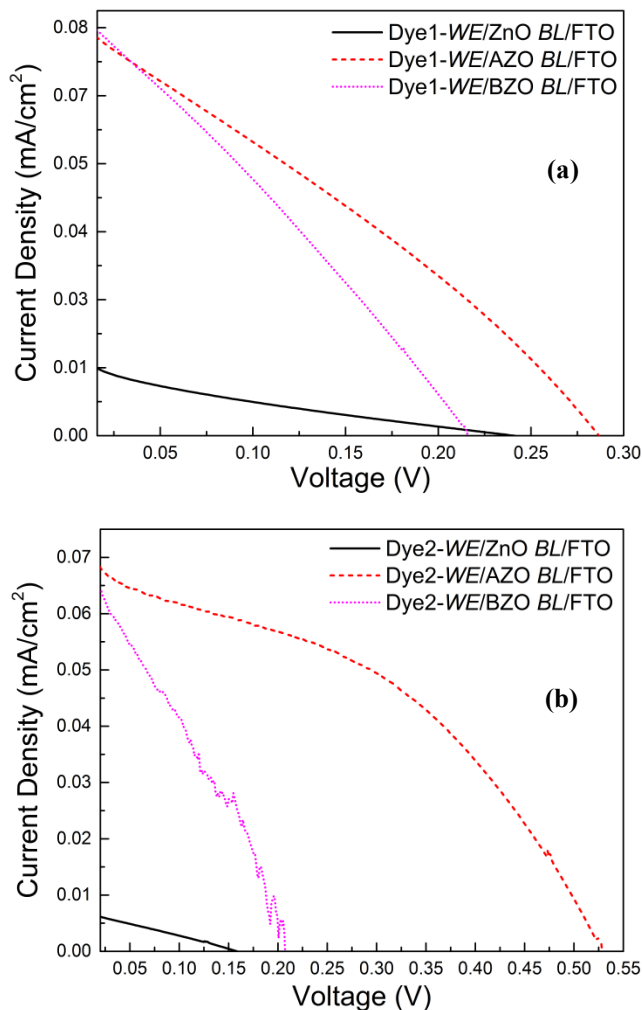


Figure 5. (b) $J-V$ characteristics of the DSSC sensitized with mahaleb cherry fruit (dye2)

undoped ZnO BL is too high and it decreases with doping. The R_s is related to the semiconductor oxide film in bulk resistance, FTO coated electrode, metallic contacts and electrolyte. Reduction in the R_s value improves the FF and so enhances cell photoelectrical characteristics [21]. The crystal quality of the materials determines the R_{sh} caused by leakage current across the interfaces of layers. Our results are consistent with the literature [21], since the findings

demonstrate that low series resistance leads to significant increase in photo current density.

Let us focus on V_{oc} now. The high V_{oc} value of the DSSCs is mainly attributed to high energy band gap. The band gap of the WEs with AZO BL is higher than that of WEs with BZO BL . It can be observed from the results that V_{oc} of DSSC with AZO BL is higher than that of DSSC with BZO BL . This result arises from the energy barrier effect and surface effectiveness of blocking layer. Moreover, the presence of doped blocking layer at the interface of TiO_2/FTO causes a noticeable increment of electron density in the conductivity band of the semiconductor layer, thus inducing improved FF and V_{oc} . The best result was found with the cell with AZO BL sensitized by mahaleb cherry fruit dye extract. This result can be ascribed to the good absorption properties of mahaleb cherry fruit extract and the low R_s value of AZO BL structure.

4. CONCLUSIONS

The photovoltaic performance of the DSSCs was enhanced by Al and B doped ZnO BLs . These BLs form an energy barrier between transparent conductive oxide and semiconductor layer, which leads to an increment in V_{oc} and FF . Furthermore, the BL prevents charge recombinations at the interfaces of layers so that photo-current density is increased. As a result, the performance of the DSSCs was improved by the presence of AZO and BZO blocking layers. Finally, our results suggested that further consideration of alternative dopants utilized for the blocking layers is necessary to boost the performance of the DSSCs.

5. ACKNOWLEDGEMENT

The authors acknowledge financial support from Ankara Yıldırım Beyazıt University Scientific Research Projects with grant number of 3746.

REFERENCES

- [1] N. Huang, Y. Liu, T. Peng, X. Sun at al. J. Pow. Sou., 204, 237 (2012),
- [2] B. O'Regan, M. Graetzel. Nature, 353, 737 (1991),
- [3] J. Ding, Y. Li, H. Hu, L. Bai et al., Nano. Res. Let., 8, 1 (2013).
- [4] Z. S. Wang, H. Kawauchi, T. Kashima, H. Arakawa, Coord. Chem. Rev., 248, 1381 (2004),
- [5] J. C. Chou, Y. J. Lin, Y. H. Liao, C. H. Lai, C. M. Chu, P. H. You, Y. H. Nien, J. Elec. Dev. Soc., 4, 402 (2016).
- [6] Y. Liu, X. Sun, Q. Tai, H. Hu, B. Chen, N. Huang, B. Sebo, X. Z. Zhao, J. Pow. Sou., 196, 475 (2010).
- [7] J. Xia, N. Masaki, K. Jiang, S. Yanagida, J. Phys. Chem. C, 111, 8092 (2007).
- [8] Y. Horie, K. Daizaka, H. Mukae, S. Guo, T. Nomiyama, Electrochim. Acta, 187, 348 (2016).
- [9] Y. Yanga et al., Ceram. Int., 40, 15199 (2014).
- [10] T. Taguchi et al., Chem. Commun., 9, 2480 (2003).

Table 1. The performance parameters for DSSCs sensitized by wild jasmine

Blocking layer	R_s (Ω)	R_{sh} (Ω)	J_{sc} (mA/cm^2)	FF (%)	V_{oc} (V)
ZnO	34618	3465	0.016	11.7	0.238
AZO	3711	4226	0.076	27.6	0.285
BZO	3417	2597	0.077	25.8	0.216

Table 2. The performance parameters for DSSCs sensitized by mahaleb cherry fruit

Blocking layer	R_s (Ω)	R_{sh} (Ω)	J_{sc} (mA/cm^2)	FF (%)	V_{oc} (V)
ZnO	31262	6928	0.006	17.8	0.157
AZO	1827	3368	0.072	35.6	0.522
BZO	3491	1449	0.066	22.6	0.211

- [11]G. Yang, Z. Yan, T. Xiao, *Appl. Surf. Sci.*, 258, 8704 (2012).
- [12]S. Ito, T. N. Mukarami, P. Comte, P. Liska, C. Graetzel, M. K. Nazeeruddin, M. Graetzel, *Thin Solid Films*, 516, 4613 (2007).
- [13]L. Sang, M. Chai, Y. Zhao, N. Ren, Y. Wu, C. Burda, *Sol. En. Mat. Sol. Cells*, 140, 167 (2015).
- [14]N. F. Djaja, D. A. Montja, R. Saleh. *Adv. Mat. Phys. Chem.*, 3, 33 (2013).
- [15]K. Mahmood, H. J. Sung, *J. Mat. Chem. A*, 2, 5408 (2014).
- [16]J. Zhang, W., Que, *Sol. En. Mat.& Sol. Cells*, 94, 2181 (2010).
- [17]R. L. Puurunen, T. Sajavaara, E. Santala, V. Miikkulainen et al., *Sens. Act. A: Phys.*, 188, 240 (2012).
- [18]J. H. Qi, Y. Li, T. T. Duong, H. J. Choi, S. G. Yoon. *J. Alloys Comp.*, 556, 121 (2013).
- [19]A. S. Gonçalves, M.S. Goes, F. Fabregat-Santiago, T. Moehl, M.R. Davolos, J. Bisquert, S. Yanagida, A.F. Nogueira, P.R. Bueno, *Electrochim. Acta*, 56, 6503 (2011).
- [20]N. S. A. Rashid, S. Suhaimi, M. M. Shahimin, M. H. A. Wahid, N. A. M. Ahmad Hambali, *ARPN J. Eng. Appl. Sci.*, 11, 4669 (2016).
- [21]H. Chen, A. D. Pasquier, G. Saraf, J. Zhong, Y. Lu, *Semi. Sci. Tech.*, 23, 045004 (2008).

